Journal of Sound and Vibration (1998) **217**(5), 807–825
Article No. 981775

NON-LINEAR DYNAMICS AND CHAOS CONTROL OF A DAMPED SATELLITE WITH PARTIALLY-FILLED LIQUID

Z.-M. Ge, C.-I. Lee, H.-H. Chen and S.-C. Lee

Department of Mechanical Engineering, *National Chiao Tung University*, *Hsinchu*, *Taiwan*, *Republic of China*

(*Received* 14 *August* 1997, *and in final form* 22 *May* 1998)

The dynamic behaviors of a damped satellite with partially-filled liquid which is subjected to external disturbance are studied in this paper. The Lyapunov direct method is used to obtain conditions of stability of the equilibrium point of the system. A co-dimension one bifurcation analysis for the autonomous system is carried out near the degenerate point. It is found that Hopf bifurcation occurs in the system by center manifold theory. By applying numerical results, phase diagrams, power spectrum, Poincaré maps, and Lyapunov exponents are presented to observe periodic and chaotic motions. The effect of the parameter changes in the system can be found in the bifurcation and parametric diagrams. For global analysis, the basins of attraction of each attractor of the system are located by employing the modified interpolated cell mapping (MICM) method. Finally, several methods, the delayed feedback control, the addition of constant motor torque, the addition of periodic force, and adaptive control algorithm are used to control chaos effectively.

1. INTRODUCTION

During the past one and a half decades, a large number of studies have shown that chaotic phenomena are observed in many physical systems that possess non-linearity [1–2]. Many studies of the satellite system partially filled with liquid have been carried out in recent years. This paper will study the non-linear behaviors of a simplified system. Because of the complexity of the problem, we assume in the analysis that liquid is solidified and the influence of the motion of the sloshing liquid on stability is simulated by an approximate moment caused by the equivalent solid. Satisfactory results were obtained which can meet requirement in applications.

The aim of this paper is to present the detailed dynamics of the satellite system partially filled with liquid. A lot of modern techniques are used in analyzing the deterministic non-linear system behavior. Both analytical and computational methods are employed to obtain the characteristics of the non-linear systems. Finally, attention is shifted to chaos control. For this purpose, the delayed feedback control, the addition of constant motor torque, the addition periodic force,and adaptive control algorithm (ACA) are used to control chaos.

0022–460X/98/450807 + 19 $30.00/0

2. EQUATIONS OF MOTION

Assume that there is a partially liquid-filled cylindrical tank in a satellite, as shown in Figure 1. Let $o\xi\eta\zeta$ be an orthogonal inertial coordinate system with origin at mass centre O of the spacecraft without liquid. Let $Oxyz$ be a rotating orthogonal coordinate system fixed with spacecraft and Ox, Oy and Oz be the three principal axes of inertia, after liquid is solidified. A, B, C are the principal moments of inertia (liquid plus rigid). G is the mass center of the system on Oz, and assume that the distance between O and G is zero. ω_1, ω_2, ω_3 are the projection of the angular velocity ω on x, y, z axis respectively. The Euler dynamic equations of system are [3]

$$\begin{aligned} A\dot{\omega}_1 + (C - B)\omega_2\omega_3 + \dot{h}_1 + \omega_2 h_3 - \omega_3 h_2 &= M_x^L \\ B\dot{\omega}_2 + (A - C)\omega_3\omega_1 + \dot{h}_2 + \omega_3 h_1 - \omega_1 h_3 &= M_y^L \\ C\dot{\omega}_3 + (B - A)\omega_1\omega_2 + \dot{h}_3 + \omega_1 h_2 - \omega_2 h_1 + b\omega_3 &= M_z^L \end{aligned} \tag{2.1}$$

where b is the damping coefficient, $O\zeta$ is vertical and upward and h_i ($i = 1, 2, 3$) is the angular momentum of rotor which is located along Ox, Oy, and Oz respectively for stabilizing the orientation of the satellite. The analysis below will be made under the following assumptions: the angular momentum of the rotor is constant, i.e., $h_i = \text{constant}$ ($i = 1, 2, 3$), resistance such as the friction drag in motion of the rotor can be neglected, solid parts of the spacecraft and the rotors are rigid bodies and the axes of rotation of the rotors are fixed on the spacecraft, and the mass of the rigid parts is symmetrical about the Oz axis, i.e., $A = B$.

Because of the complexity of the problem, it is generally difficult to determine the internal slosh moment. To simplify the problem and make it easier to study,

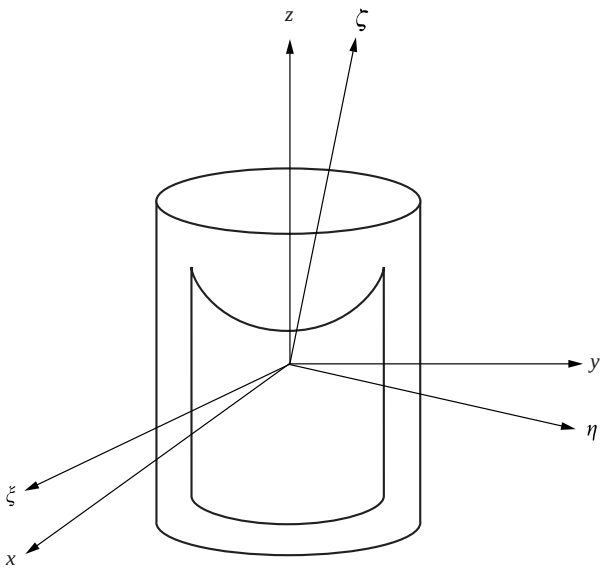

Figure 1. Physical model of the system.

we solidify the liquid and add the internal moment to the system as an external moment. Assume that

$$M_x^L = \mu_{xy}\omega_2$$
$$M_y^L = \mu_{yx}\omega_1$$
$$M_z^L = 0 \tag{2.2}$$

where μ_{xy} μ_{yx} are coefficients influenced by many factors about sloshing. Equation (2.1) is rewritten as follows:

$$A\dot{\omega}_1 + (C - B)\omega_2\omega_3 + \omega_2 h_3 - \omega_3 h_2 = \mu_{xy}\omega_2$$
$$B\dot{\omega}_2 + (A - C)\omega_3\omega_1 + \omega_3 h_1 - \omega_1 h_3 = \mu_{yx}\omega_1$$
$$C\dot{\omega}_3 + (B - A)\omega_1\omega_2 + \omega_1 h_2 - \omega_2 h_1 + b\omega_3 = 0. \tag{2.3}$$

3. STABILITY ANALYSIS BY LYAPUNOV DIRECT METHOD

The stability of the system will be investigated by the Lyapunov direct method [4]. In this section, first the only equilibrium of the system can be found from equation (2.3) as $p = (0, 0, 0)$. Add slight disturbances x, y, z to the fixed point (0, 0, 0)

$$\omega_1 = x, \qquad \omega_2 = y, \qquad \omega_3 = z. \tag{3.1}$$

Substitute equation (3.1) into equation (2.3); it becomes

$$x = \left(1 - \frac{C}{A}\right)yz + \frac{h_2}{A}z - \frac{h_3}{A}y + \frac{\mu_{xy}}{A}y$$

$$y = -\left(1 - \frac{C}{A}\right)xz + \frac{h_3}{A}x - \frac{h_1}{A}z + \frac{\mu_{yx}}{A}x$$

$$z = -\frac{h_2}{C}x + \frac{h_1}{C}y - \frac{b}{C}z. \tag{3.2}$$

Construct a Lyapunov function as:

$$V = x^2 + y^2 + \frac{C}{A}z^2 + xy + xz. \tag{3.3}$$

By Sylvester's theorem [4], the sufficient condition for the positive definiteness of function V is

$$\frac{C}{A} > \tfrac{1}{3} \tag{3.4}$$

and the time derivative of V through equation (3.2) is

$$\frac{\mathrm{d}V}{\mathrm{d}t} = a_{11}x^2 + a_{22}y^2 + a_{33}z^2 + 2a_{12}xy + 2a_{23}yz + 2a_{13}xz + \cdots \tag{3.5}$$

where ellipsis dots are high order terms and

$$a_{11} = \frac{\mu_{yx} + h_3}{A} - \frac{h_2}{C}, \qquad a_{22} = \frac{\mu_{xy} - h_3}{A}, \qquad a_{33} = \frac{h_2 - b}{A}$$

$$a_{12} = \frac{\mu_{xy} + \mu_{yx}}{A} + \frac{h_1}{2C}, \qquad a_{23} = \frac{h_2 + \mu_{xy} - h_3}{2A}, \qquad a_{13} = \frac{-h_1}{2A} - \frac{b}{2C}.$$

By Sylvester's theorem, the time derivative of V is negative definite if

$$a_{11} < 0$$

$$a_{11}a_{22} - a_{12}^2 > 0$$

$$a_{11}a_{22}a_{33} + 2a_{12}a_{13}a_{23} - a_{11}a_{23}^2 - a_{22}a_{13}^2 - a_{33}a_{12}^2 < 0. \tag{3.6}$$

The conditions of the stability of the satellite system are the three inequalities in equation (3.6). If we choose $A = 500$, $C = 1000$, $h_2 = 1200$, $h_3 = 300$, $\mu_{xy} = \mu_{yx} = 50$, from equation (3.6) the system is stable when $h_1 < -616{\cdot}2$.

4. APPLICATION OF CENTER MANIFOLD THEORY

In non-linear dynamical systems, variation of system parameters may cause a sudden change in the qualitative behavior of their state. The state change is referred to as a bifurcation and the parameter value at which the bifurcation occurs is called the bifurcation point [5]. Here we give attention to that Hopf bifurcation will occurs in this system [6]. We assume $h_1 = h_2$ and $\mu_{xy} = \mu_{yx}$ to simplify the system. Equation (3.2) is rewritten in matrix form

$$\dot{X} = PX + f(X), \qquad X \in R^3 \tag{4.1}$$

where

$$X = [x, y, z]^{\mathrm{T}}$$

$$P = \begin{bmatrix} 0 & \dfrac{\mu_{xy} - h_3}{A} & \dfrac{h_1}{A} \\ \dfrac{h_3 + \mu_{xy}}{A} & 0 & \dfrac{-h_1}{A} \\ \dfrac{-h_1}{C} & \dfrac{h_1}{C} & \dfrac{-b}{C} \end{bmatrix}$$

$$f = \begin{bmatrix} f_1(X) \\ f_2(X) \\ 0 \end{bmatrix}$$

where

$$f_1(X) = \left(1 - \frac{C}{A}\right)yz, \qquad f_2(X) = -\left(1 - \frac{C}{A}\right)xz.$$

The Jacobian matrix P is evaluated at the fixed point $(0, 0, 0)$. Further, it is necessary to find the value of μ_{xy} for which the eigenvalues of P contain a pure imaginary pair and the remaining eigenvalue has negative real part. The conditions for a pure imaginary pair of eigenvalues can be shown to be

$$\mu_{xy} = -\frac{bA}{C}.$$

The system has pure imaginary eigenvalues

$$\pm \mathrm{i}\sqrt{\frac{h_3^2}{A^2} + \frac{2h_1^2}{AC} - \frac{b^2}{C^2}} = \pm \mathrm{i}\xi$$

and that the third eigenvalue is $-b/C$.

At this critical parameter μ_{xy}, the origin is non-hyperbolic. The eigenvalues of matrix P fails to determine the stability of the fixed point and it becomes necessary to consider the higher order terms to analyze the three-dimensional non-linear system. So we use the following method to analyze the dynamical system. First, the center manifold theorem will be applied to reduce the dimension of the state spaces at the critical parameter μ_{xy}. The following linear transformation matrix is used to transform equation (4.1):

$$T = \begin{bmatrix} 1 & -\dfrac{b}{C} - \dfrac{h_3}{A} & h_1 \\ -1 & \dfrac{b}{C} - \dfrac{h_3}{A} & h_1 \\ 0 & \dfrac{2h_1}{C} & h_3 \end{bmatrix}$$

which is formed by eigenvectors of P. It can be evaluated that

$$T^{-1} = \frac{1}{\Delta}\begin{bmatrix} \dfrac{Abh_3 - Ch_3^2 - 2Ah_1^2}{A^2C} & \dfrac{Abh_3 + Ch_3^2 + 2Ah_1^2}{A^2C} & \dfrac{-2bh_1}{AC} \\ \dfrac{h_3}{A} & \dfrac{h_3}{A} & \dfrac{-2h_1}{A} \\ \dfrac{-2h_1}{C} & \dfrac{-2h_1}{C} & \dfrac{-2h_3}{A} \end{bmatrix}$$

$$\Delta = \frac{-2Ch_3^2 - 4Ah_1^2}{A^2C}.$$

Let

$$\begin{bmatrix} x \\ y \\ z \end{bmatrix} = T \begin{bmatrix} q_1 \\ q_2 \\ q_3 \end{bmatrix}$$

then equation (4.1) is transformed into Jordan form

$$\begin{bmatrix} \dot{q}_1 \\ \dot{q}_2 \\ \dot{q}_3 \end{bmatrix} = \begin{bmatrix} 0 & -\xi & 0 \\ \xi & 0 & 0 \\ 0 & 0 & \dfrac{-b}{C} \end{bmatrix} \begin{bmatrix} q_1 \\ q_2 \\ q_3 \end{bmatrix} + T^{-1} f(Tq) \tag{4.2}$$

where

$$f(Tq) = \left(1 - \frac{C}{A}\right)$$

$$\begin{bmatrix} -\dfrac{2h_1}{C} q_1 q_2 + \dfrac{2h_1}{C}\left(\dfrac{b}{C} - \dfrac{h_3}{A}\right) q_2^2 + \left(\dfrac{2h_1^2 + bh_3}{C} - \dfrac{h_3^2}{A}\right) q_2 q_3 + h_3 q_1 q_3 + h_1 h_3 q_3^2 \\ -\dfrac{2h_1}{C} q_1 q_2 + \dfrac{2h_1}{C}\left(\dfrac{b}{C} + \dfrac{h_3}{A}\right) q_2^2 + \left(\dfrac{-2h_1^2 + bh_3}{C} + \dfrac{h_3^2}{A}\right) q_2 q_3 - h_3 q_1 q_3 - h_1 h_3 q_3^2 \\ 0 \end{bmatrix}.$$

According to the center manifold theory, it is found that there exists a center manifold tangent to the two-dimensional eigenspace which is spanned by the eigenvectors corresponding to the pure imaginary pair eigenvalues. The behavior of the original system in close vicinity to the degenerate point can be determined by a two-dimensional system restricted within the center manifold $h(q_1, q_2)$ [7]. We have

$$\begin{bmatrix} \dot{q}_1 \\ \dot{q}_2 \end{bmatrix} = \begin{bmatrix} 0 & -\xi \\ \xi & 0 \end{bmatrix} \begin{bmatrix} q_1 \\ q_2 \end{bmatrix} + \begin{bmatrix} f_1(q) \\ f_2(q) \end{bmatrix} \tag{4.3}$$

where

$$f_2(q) = \frac{A-C}{\Delta A}\left\{\frac{-4bh_1h_3}{AC^2}\,q_1q_2 + \left(\frac{4b^2h_1h_3}{AC^3} + \frac{4Ah_1^2h_3 + 2Ch_3^3}{A^3C}\right)q_2^2\right.$$

$$+ \left[\frac{2b^2h_3^2}{AC^2} + \left(\frac{Ch_3^2 + 2Ah_1^2}{A^2C}\right)\left(\frac{2Ch_3^2 - 4Ah_1^2}{AC}\right)\right]\left[(C^2\xi + 2C^2\xi^2)q_1^2q_2\right.$$

$$\left. - \left(\frac{b^3 - bC^2\xi + 2bC^2\xi^2}{C\xi}\right)q_1q_2^2 + (b^2 - C^2\xi + 2C^2\xi^2)q_2^3\right]$$

$$- \left(\frac{2Ch_3^3 + 4Ah_1^2h_3}{A^2C}\right)\left[(C^2\xi + 2C^2\xi^2)q_1^3 - \left(\frac{b^3 - bC^2\xi + 2bC^2\xi^2}{C\xi}\right)q_1^2q_2\right.$$

$$\left. + (b^2 - C^2\xi + 2C^2\xi^2)q_1q_2^2\right] - \left(\frac{2h_1h_3^3 + 4Ah_1^3h_3}{A^2C}\right)\left[(C^2\xi + 2C^2\xi^2)q_1^2\right.$$

$$\left.\left. - \left(\frac{b^3 - bC^2\xi + 2bC^2\xi^2}{C\xi}\right)q_1q_2 + (b^2 - C^2\xi + 2C^2\xi^2)q_2^2\right]^2\right\}$$

$$f_2(q) = \frac{A-C}{\Delta A}\left\{-\frac{4h_1h_3}{AC}\,q_1q_2 + \frac{4h_1h_3b}{AC^2}\,q_2^2 + \frac{2bh_3^2}{AC}\,(C^2\xi + 2C^2\xi^2)q_1^2q_2\right.$$

$$\left. - \left(\frac{b^3 - bC^2\xi + 2bC^2\xi^2}{C\xi}\right)q_1q_2^2 + (b^2 - C^2\xi + 2C^2\xi^2)q_3^2\right\}$$

and the center manifold is

$$h(q_1, q_2) = (C^2\xi + 2C^2\xi^2)q_1^2 - \left(\frac{b^3 - bC^2\xi + 2bC^2\xi^2}{C\xi}\right)q_1q_2$$

$$+ (b^2 - C^2\xi + 2C^2\xi^2)q_2^2. \tag{4.4}$$

The Hopf bifurcation stability formula for a general two-dimensional system of equation (4.3) is:

$$a = \frac{1}{16}\left(\frac{\partial^3 f_1}{\partial q_1^3} + \frac{\partial^3 f_1}{\partial q_1\,\partial q_2^2} + \frac{\partial^3 f_1}{\partial q_1^2\,\partial q_2} + \frac{\partial^3 f_1}{\partial q_2^3}\right) + \frac{1}{16\omega}\left[\frac{\partial^2 f_1}{\partial q_1\,\partial q_2}\left(\frac{\partial^2 f_1}{\partial q_1^2} + \frac{\partial^2 f_1}{\partial q_2^2}\right)\right.$$

$$\left. - \frac{\partial^2 f_2}{\partial q_1\,\partial q_2}\left(\frac{\partial^2 f_2}{\partial q_1^2} + \frac{\partial^2 f_2}{\partial q_2^2}\right) - \frac{\partial^2 f_1}{\partial q_1^2}\frac{\partial^2 f_2}{\partial q_1^2} + \frac{\partial^2 f_1}{\partial q_2^2}\frac{\partial^2 f_2}{\partial q_2^2}\right]. \tag{4.5}$$

In our case, we obtain that

$$a = \frac{1}{16\Delta}\left(1 - \frac{C}{A}\right)\left\{-\frac{(2Ch_3^3 + 4h_1^2h_3)(b^2 + 4C^2\xi^2)}{A^2C} + \left[\frac{2b^2h_3^2}{AC^2}\right.\right.$$

$$\left.\left. + \frac{(Ch_3^2 + 2Ah_1^2)(2Ch_3^2 + 4Ah_1^2)}{A^3C^2}\right]\left(\frac{-b^3 + bC^2\xi - 2bC^2\xi^2}{C\xi}\right)\right.$$

$$\left. + \frac{2bh_3^2(b^2 + 4C^2\xi^2)}{AC}\right.$$

$$\left. + \frac{1}{16\omega\Delta^2}\left(1 - \frac{C}{A}\right)^2\left(\frac{16bh_1^2h_3^2}{A^2C^3}\right)\right. . \tag{4.6}$$

If $a < 0$, the periodic orbits are stable and occur above bifurfation (supercritical), while if $a > 0$, they are unstable and occur below bifurcation (subcritical). The system is always stable with the given parameters: $A = 500$, $C = 1000$, $h_2 = 1200$, $h_3 = 300$, $\mu_{xy} = \mu_{yx} = 50$.

5. PHASE PORTRAITS, POINCARÉ MAP AND POWER SPECTRUM

In previous sections, the angular momentum of rotor h_3 is assumed to be constant for the system. Another condition can be considered. The angular momentum of rotor h_3 is now not constant but is represented by a constant term and a harmonic term $h_3(1 + a \sin \omega t)$, where h_3, a, ω are constants. The equation (3.2) is rewritten in the form

$$\dot{x} = \left(1 - \frac{C}{A}\right)yz + \frac{h_2}{A}z - \frac{h_3(1 + a\cos\omega t)}{A}y + \frac{\mu_{xy}}{A}y$$

$$\dot{y} = -\left(1 - \frac{C}{A}\right)xz + \frac{h_3(1 + a\cos\omega t)}{A}x - \frac{h_1}{A}z + \frac{\mu_{yx}}{A}x$$

$$\dot{z} = -\frac{h_2}{C}x + \frac{h_1}{C}y - \frac{b}{C}z + \frac{h_3 a \sin\omega t}{C} \tag{5.1}$$

where $A = 500$, $C = 1000$, $\mu_{xy} = \mu_{yx} = 50$, $h_1 = h_2 = 200$, $h_3 = 250$, $b = 200$, $\omega = 1{\cdot}0$ [3].

The phase portrait is the evolution of a set of trajectories emanating from various initial conditions in the state space. When the solution reaches steady state, the transient behavior disappears. The idea of transforming the study of continuous systems into the study of an associated discrete system was presented by Henri Poincaré [8]. One of the many advantages of the Poincaré map is to reduce dimensions of the dynamical system [9]. The technique introducced by Poincaré deals with the question with the four-dimensional phase space (x, y, z, t) whenever t is a multiple of $T = 2\pi/\omega$. Here T is the period of the external torque.

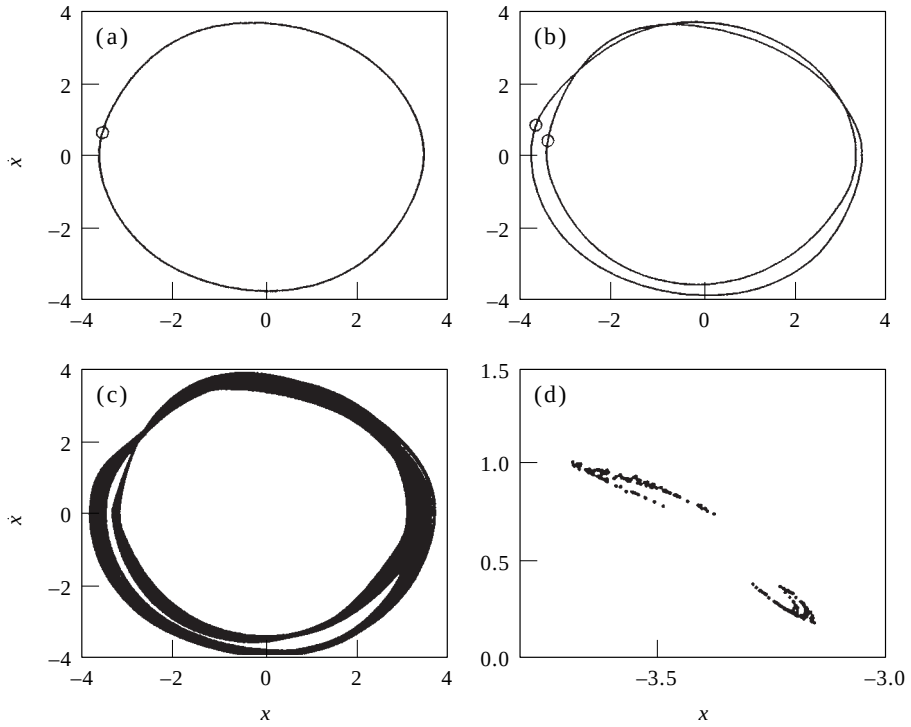

Figure 2. Phase portraits and Poincaré map for (a) $a = 14{\cdot}6$, (b) $a = 14{\cdot}4$, (c) phase portraits for $a = 14{\cdot}2$ and (d) Poincaré map for $a = 14{\cdot}2$.

A similar trajectory bundle emerges from each $t = mT$ plane ($m = 0, 1, 2, 3, \ldots$.) so that photographs of every interval would be identical. The solution of period-1T in the phase plane will become one point in the Poincaré map. By using the fourth order Runge–Kutta numerical integration method, the phase plane and Poincaré map of the satellite system, equation (5.1), is plotted in Figure 2(a), (b) for $a = 14{\cdot}6$ and $14{\cdot}4$ respectively. Clearly, the motion is periodic. But Figure 2(c), (d) for $a = 14{\cdot}2$ show the chaotic state. Because the Poincaré map is neither a finite set of points nor a closed orbit, the motion may be chaotic.

Any function $x(t)$ may be represented as a superposition of different periodic components. The determination of their relative strength is called spectral analysis. Due to the character of the function $x(t)$, there are two different methods to express $x(t)$. If it is periodic, the spectrum may be a linear combination of oscillations whose frequencies are integer multiples of a basic frequency. The linear combination is called a Fourier series. If it is not periodic, the spectrum then must be in terms of oscillations with a continuum of frequencies. Such a representation of the spectrum is called Fourier integral of $x(t)$. This representation is useful for dynamical analysis. The nonautonomous system is observed by the portraits of time history and power spectrum for $a = 14{\cdot}6$. In Figure 3(a), the solution of system is period-1T, and the power spectrum exhibits a strong peak at the forcing frequency together with super-harmonic frequencies. As the a increases, the period-1T changes to period-2T and the peak arises at one half forcing frequency, twice the principal period in the power spectrum.

Apparently, the spectrum of the periodic motion only consists of discrete frequencies. As $a = 14{\cdot}2$ chaos occurs, the points of Poincaré map become obviously irregular. The spectrum is a broad band and the peak is still presented at the fundamental frequency shown in Figure 3(b). The noise-like spectrum is the characteristic of chaotic dynamical system.

6. BIFURCATION DIAGRAM AND PARAMETRIC DIAGRAM

In the previous section, the information about the dynamics of the non-linear system for specific values of the parameters is provided. The dynamics may be viewed more completely over a range of parameter value. As the parameter is changed, the equilibrium points can be created or destroyed, or their stability can be lost. The phenomenon of sudden change in the motion as a parameter is varied is called bifurcation, and the parameter values at which they occur are called bifurcation points.

The bifurcation diagram of the non-linear system of equation (5.1) is depicted in Figure 4. It is calculated by the fourth order Runge–Kutta numerical integration and plotted against $a \in [14{\cdot}2, 14{\cdot}6]$, while the incremental value of a is $0{\cdot}005$. At each a, the points of the Poincaré map for the transient state of motion are discarded. Figure 4 presents the amplitude of the angular momentum of the rotor which is located along the Oz axis versus angular velocity.

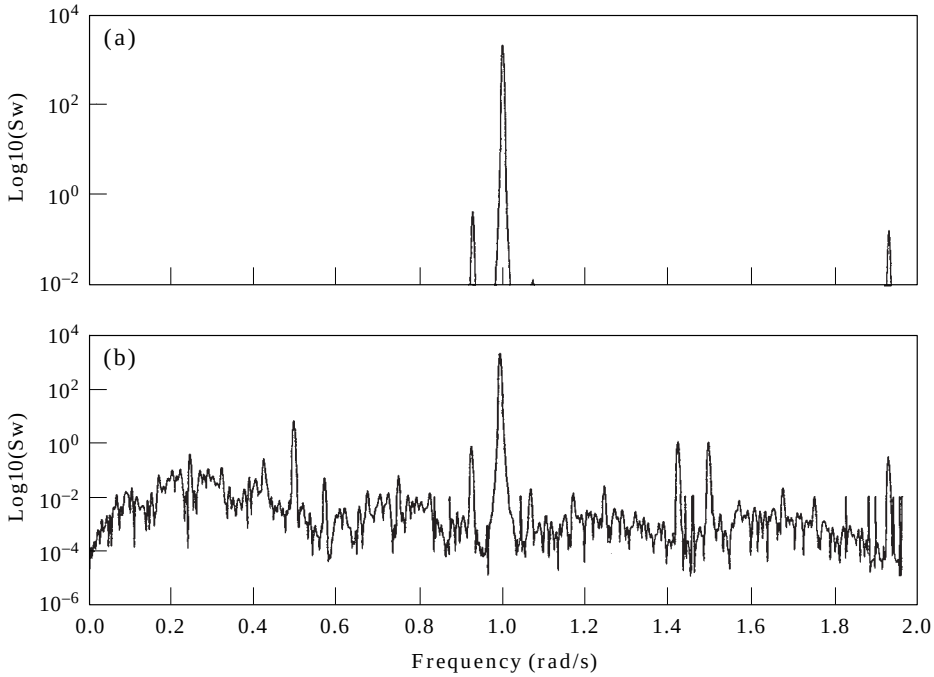

Figure 3. Power spectrum for (a) $a = 14{\cdot}6$ and (b) $a = 14{\cdot}2$.

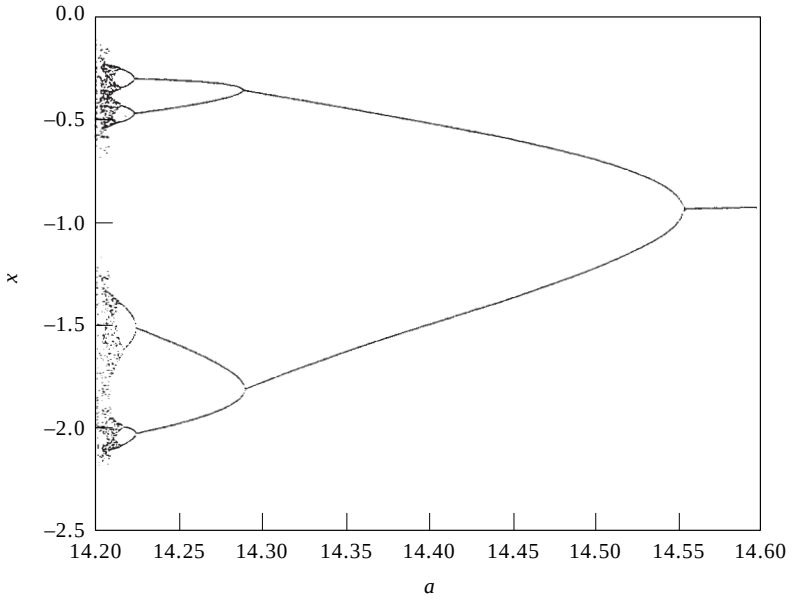

Figure 4. Bifurcation diagram of a versus angular velocity.

Further, the parameter values, damping coefficient and forcing frequency will also be varied to observe the behaviors of bifurcation of the system. By varying simultaneously any two of the three parameters, amplitude of the external torque, damping coefficient, and forcing frequency, the parametric diagrams are described and shown as in Figure 5(a), (b). The enriched information of the behaviors of the system can be obtained from the diagrams. In Figure 5(a), when the amplitude increases, the periodic and chaotic motion alternate with each other. We can find that the region of chaos includes the period-3 region from Figure 5(b). Obviously, ''period-3 implies chaos'' was presented.

7. LYAPUNOV EXPONENT AND LYAPUNOV DIMENSION

The Lyapunov exponent may be used to measure the sensitive dependence upon initial conditions [10, 11]. It is an index for chaotic behavior. Different solutions of the dynamical system, such as fixed points, periodic motions, quasiperiodic motion, and chaotic motion can be distinguished by it. If two chaotic trajectories start close to one another in phase space, they will move exponentially away from each other for small times on the average. Thus, if d_0 is a measure of the initial distance between the two starting points, the distance is $d(t) = d_0 2^{\lambda t}$. The symbol λ is called Lyapunov exponent. The divergence of chaotic orbits can only be locally exponential, because if the system is bounded, $d(t)$ cannot grow to infinity. A measure of this divergence of orbits is that the exponential growth at many points along a trajectory has to be averaged. When $d(t)$ is too large, a new 'nearby' trajectory $d_0(t)$ is defined. The Lyapunov exponent can be expressed as:

$$\lambda = \frac{1}{t_N - t_0} \sum_{k=1}^{N} \log_2 \frac{d(t_k)}{d_0(t_{k-1})}. \tag{7.1}$$

The signs of the Lyapunov exponents provide a qualitative picture of a system dynamics. The criterion is

$$\lambda > 0 \quad \text{(chaotic)},$$

$$\lambda \leqslant 0 \quad \text{(regular motion)}.$$

The periodic and chaotic motions can be distinguished by the bifurcation diagram, while the quasiperiodic motion and chaotic motion may be confused. However, they can be distinguished by the Lyapunov exponent method. The

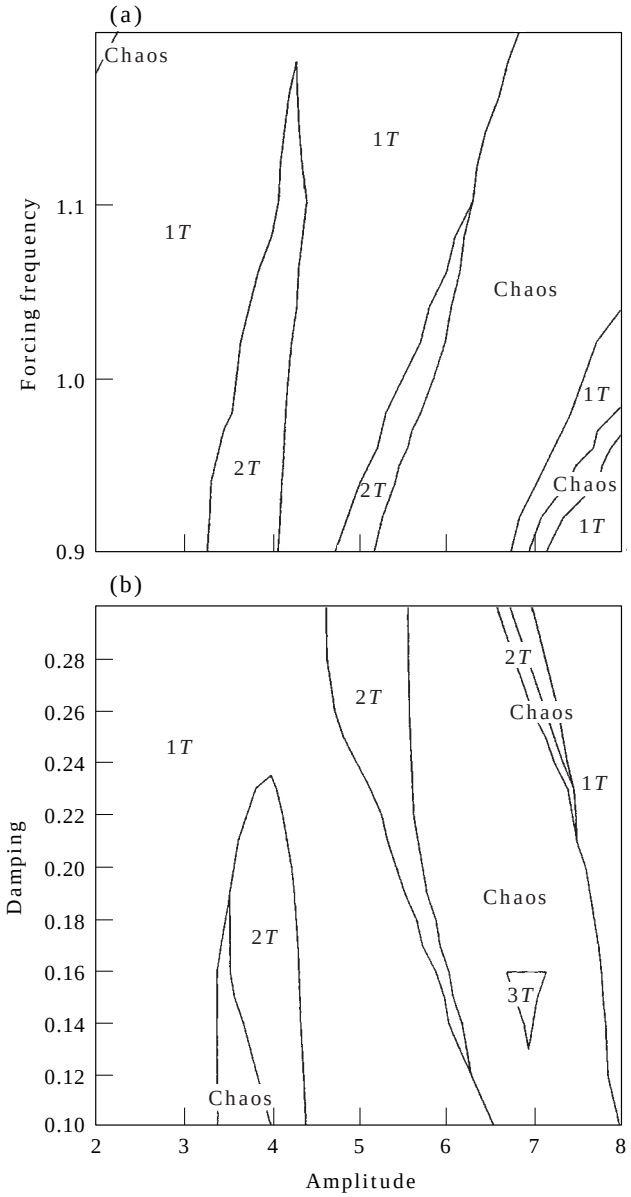

Figure 5. Parametric diagram (a) a versus ω and (b) a versus b.

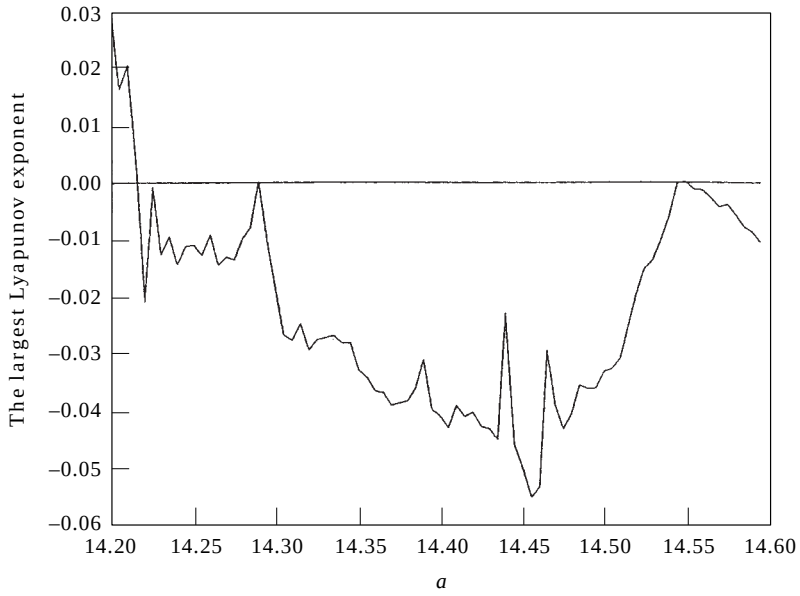

Figure 6. The largest Lyapunov exponents for a between 14·2 and 14·6.

Lyapunov exponents of the solutions of the non-linear dynamical system, equation (5.1), are plotted in Figure 6 as a ranges from 14·2 to 14·6. For the system studied the sum of the four Lyapunov exponents is equivalent to the negative damping coefficient $-0{\cdot}2$. If the value of the Lyapunov exponent is greater than zero, it is chaos; otherwise it would be periodic solution. Observably, the chaotic motion can be found in Figure 6 for a close 14·2.

There are a number of different fractional-dimension-like quantities, including the information dimension, Lyapunov dimension, and the correlation exponent, etc; the difference between them is often small. The Lyapunov dimension is a measure of the complexity of the attractor. It has been developed by Kaplan and Yorke [12] that the Lyapunov dimension d_L is introduced as

$$d_L = j + \frac{\sum_{i=1}^{j} \lambda_i}{|\lambda_{j+1}|}, \tag{7.2}$$

TABLE 1

Lyapunov exponents and Lyapunov dimensions of the system for different a

a	λ_1	λ_2	λ_3	λ_4	$\Sigma\lambda_i$	d_L	
14·58	−0·0056	0	−0·0498	−0·1446	−0·2	1	Period-1
14·4	−0·0407	0	−0·0751	−0·0842	−0·2	1	Period-2
14·25	−0·0109	0	−0·0310	−0·1581	−0·2	1	Period-4
14·223	−0·0020	0	−0·0536	−0·1444	−0·2	1	Period-8
14·2	−0·0295	0	−0·0516	−0·1779	−0·2	2·5717	Chaos

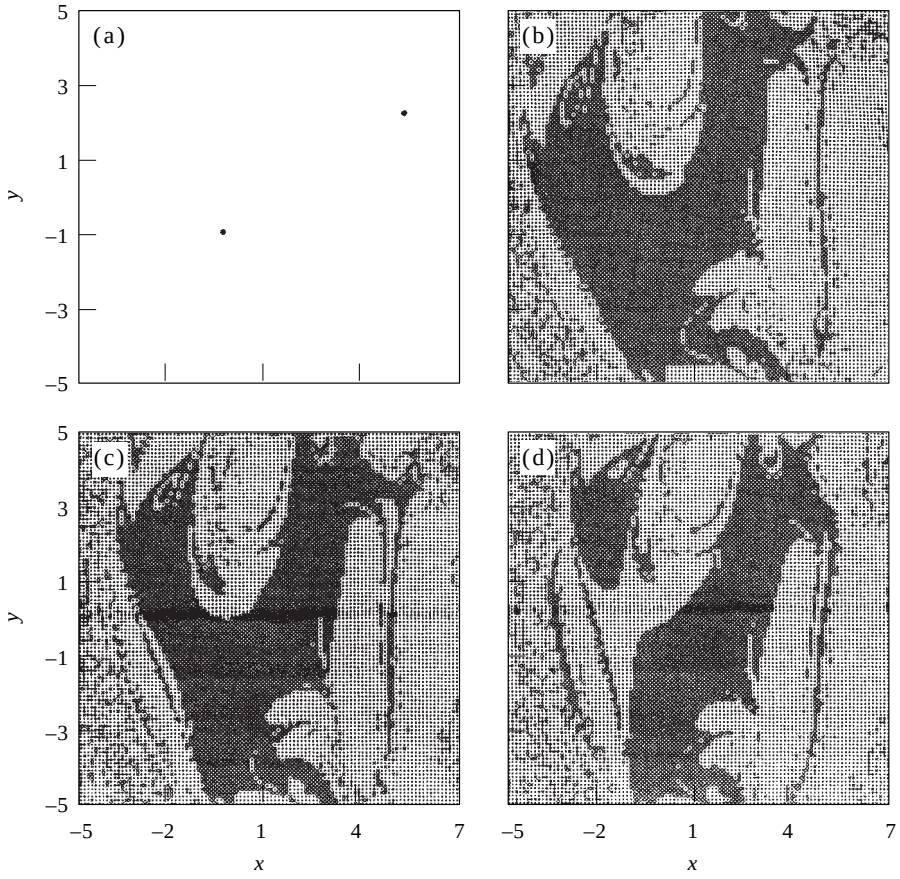

Figure 7. (a) The projection of attractors. (b) Basins of attraction for $z = 0{\cdot}9$. (c) $z = 1{\cdot}0$. (d) $z = 1{\cdot}1$.

where j is defined by the condition that

$$\sum_{i=1}^{j} \lambda_i > 0 \qquad \text{and} \qquad \sum_{i=1}^{j+1} \lambda_i < 0.$$

The Lyapunov dimension for a strange attractor is a non-integer number. The Lyapunov dimension and the Lyapunov exponent of the non-linear system are listed in Table 1 for different values of a.

8. GLOBAL ANALYSIS BY MODIFIED INTERPOLATED CELL MAPPING METHOD

A brief introduction of the modified interpolated mapping method [13] is given as follows. Consider a point mapping system which is governed by

$$X_{n+1} = f(X_n), \qquad X \in R^3 \tag{8.1}$$

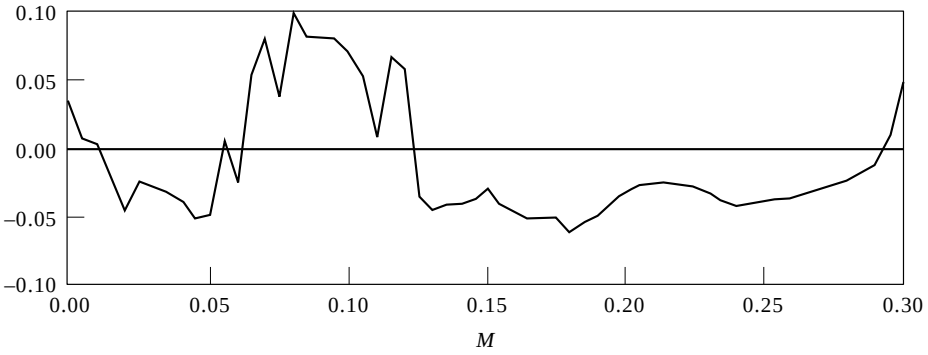

Figure 9. The largest Lyapunov exponent against M.

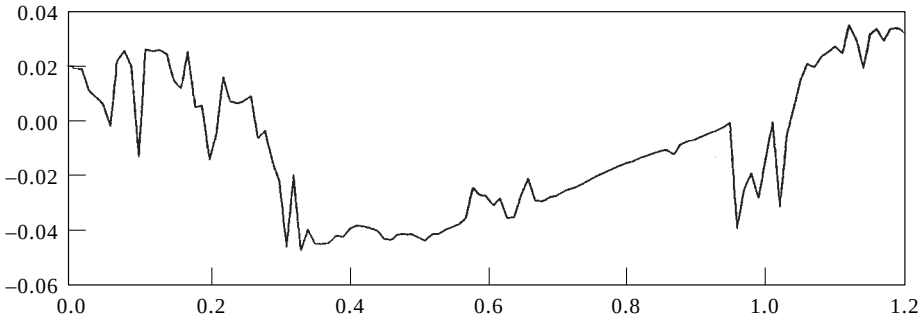

Figure 10. The largest Lyapunov exponent against a.

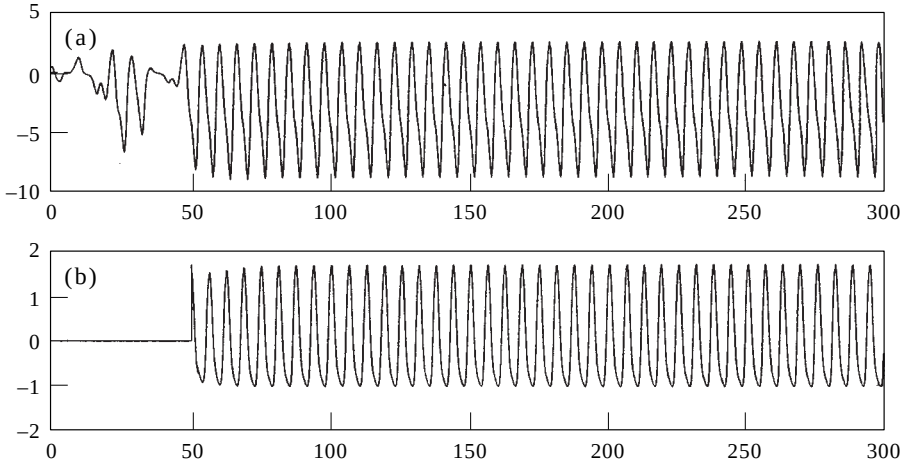

Figure 8. (a) The output signal of the system. (b) The input signal.

where $f: R^3 \to R^3$ and n is integer. The basic concept of the interpolated mapping method is to find the image X_{n+1} by using an interpolation procedure instead of the system. For a three-dimensional system, the interested region D is specified by a Cartesian product $[x_{1\,\min}, x_{1\,\max}] \times [x_{2\,\min}, x_{2\,\max}] \times [x_{3\,\min}, x_{3\,\max}]$, which is divided into $N_1 \times N_2 \times N_3$ cells. The size of the cells is $h_i = (x_{i\,\max} - x_{i\,\min})/N_i$, $i = 1, 2, 3$.

The first mappings of cells in the region of interest are constructed by numerical integration to serve as the reference mappings for the interpolation. The interpolated mapping of each cell is constructed within the mapping periods assigned, such as 30 periods. Through these mapping sequences, periodic attractors with periods of less than 30 are located by the criterion 10^{-5} cell size. If no periodic attractor is located, the 30th mapping of each cell is assigned to the first mapping, and then iterated forward to construct the next iteration of 30 mappings. If periodic attractors are located and a cell leads to a periodic attractor within the criterion 10^{-2} cell size, the cell is considered in the basin of attraction of the attractor.

For a three-dimensional system, 101^3 cells are studied by a modified interpolated mapping method, where 101 is the number of the total cells divided in each dimensional of the region of interest.

In this section the equation (5.1) with the values of parameters is considered as follows:

$$\begin{aligned} \dot{x} &= -yz + 0{\cdot}4z + 0{\cdot}1y + 0{\cdot}5(1 + a\cos\tau)y \\ \dot{y} &= xz - 0{\cdot}4z + 0{\cdot}1x + 0{\cdot}5(1 + a\cos\tau)x \\ \dot{z} &= -0{\cdot}2x + 0{\cdot}2y - 0{\cdot}2z + 0{\cdot}25a\sin\tau. \end{aligned} \tag{8.2}$$

Two black dots in Figure 7(a) for $a = 14{\cdot}6$ indicate the system motion is period-1 motion and the corresponding basins of attraction are shown in Figure 7(b–d) with $z = 0{\cdot}9$, $1{\cdot}0$, $1{\cdot}1$. The symbol "$\bigcirc$" and "$\times$" denote the cells attracted by different period-1 stable solutions. The transition from one basin of attraction to another is labelled as basin boundary. It implies that when the input parameters are away from the boundary, small uncertainties in the parameters will not affect the outcome.

9. CONTROLLING CHAOS

Several interesting non-linear dynamic behaviors of the system have been discussed in previous sections. It has been shown that the forced system exhibited both regular and chaotic motion. Usually chaos is unwanted or undesirable.

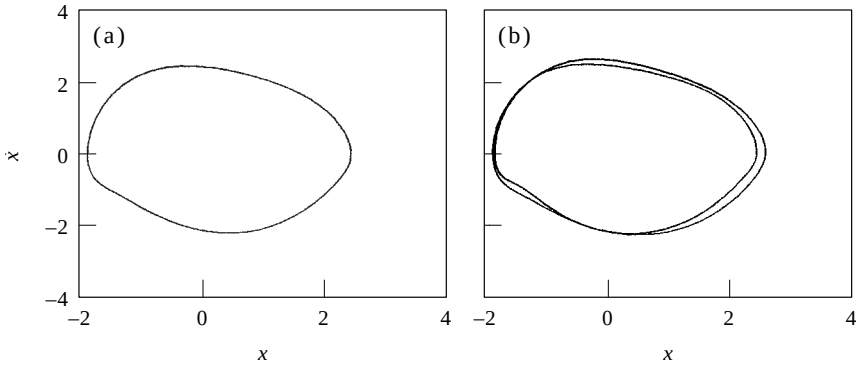

Figure 11. Phase portraits of periodic motion (a) period-1 and (b) period-2.

In order to improve the performance of a dynamic system or avoid the chaotic phenomena, we need to control a chaotic motion to become a periodic motion which is beneficial for working with a parrticular condition. It is thus of great practical importance to develop sutiable control methods. Very recently much interest has been focused on this type of problem—controlling chaos [14-17]. For this purpose, the delayed feedback control, the addition of constant motor torque, the addition periodic force, and adaptive control algorithm (ACA) are used to control chaos. As a result, the chaotic motion can be controlled.

(A) CONTROLLING OF CHAOS BY DELAYED FEEDBACK CONTROL

Let us consider a dynamic system which can be simulated by ordinary differential equations. We imagine that the equations are unknown, but some scalar variable can be measured as a system output. The idea of this method, is that the difference $D(t)$ between the delayed output signal $y(t-\tau)$ and the output signal $y(t)$ is used as a control signal. In other words, we adapt a perturbation of the form:

$$F(t) = K[\, y(t-\tau) - y(t)] = KD(t). \tag{9.1}$$

Here τ is a delay time. By choosing an appropriate weight K and τ of the feedback one can achieve the periodic state. For $K = 0{\cdot}1$ and $\tau = 2$, the results of equation (8.2) are shown in Figure 8.

This control is achieved by the use of the output signal, which is fed in a special form into the system. The difference between the delayed output signal and the output signal itself is used as a control signal. Only a simple delay line is required for this feedback control. To achieve the periodic motion of the system, two parameters, namely, the time of delay τ and the weight K of the feedback, should be adjusted.

(B) CONTROLLING OF CHAOS BY ADDITION OF CONSTANT MOTOR TORQUE

Interestingly, one can even add just a constant term to control or quench the chaotic attractor to a desired periodic one in a typical non-linear nonautonomous system. It ensures effective control in a very simple way. In order to understand this simple controlling approach in a better way, this method is applied numerically (8.2). We add the constant motor torque M into the third equation of equation (8.2).

In the absence of the constant motor torque, the system exhibits chaotic behavior under the parameter condition: $a = 14{\cdot}2$.

If one considers the effect of the constant motor torque M by increasing it from zero upwards, the chaotic behavior is then altered. Spectral analysis of the Lyapunov exponents have proven to be the most useful dynamical diagnostic tool for examining chaotic motions. In Figure 9, the maximal Lyapunov exponents are shown. It is clear that the system returns to regular motion, when the constant motor torque M is presented at certain intervals.

(C) CONTROLLING OF CHAOS BY THE ADDITION OF PERIODIC FORCE

One can control system dynamics by the addition of external periodic force in the chaotic state. For our purpose, the added periodic force, $a \sin(\bar{\omega}t + \phi)$, is

given. The system can then be investigated by numerical solution, with the remaining parameter fixed. We examine the change in the dynamics of the system as a function of a for fixed $\bar{\omega} = 1{\cdot}5$, $\phi = 0$. The maximal Lyapunov exponents are estimated numerically, and the results are shown in Figure 10. At certain intervals, the maximal Lyapunov exponents $\lambda_i \leqslant 0$, which indicates that predictability of the system recovers.

(D) CONTROLLING CHAOS BY ADAPTIVE CONTROL ALGORITHM (ACA)

Recently Huberman and Lumer [17] have suggested a simple and effective adaptive control algorithm which utilizes an error signal proportional to the difference between the goal output and actual output of the system. The error signal governs the change of parameters of the system, which readjusts so as to reduce the error to zero. This method can be explained briefly: the system motion is set back to a desired state X_s by adding dynamics on the control parameter P through the evolution equation,

$$P = \varepsilon G(X - X_s), \tag{9.2}$$

where the function G depends on the difference between X_s and the actual output X, and ε indicates the stiffness of the control. The function G could be either linear or non-linear. In order to convert the dynamics of system (8.2) from chaotic motion to the desired periodic motion (X_s), the chosen parameter a is perturbed as

$$a = \varepsilon(X - X_s). \tag{9.3}$$

If $\varepsilon = 0{\cdot}2$, the system can reach the period-1 and period-2 easily shown as Figure 11(a), (b). It is clear that the desired periodic motion can be reached by adaptive control algorithm.

10. CONCLUSIONS

The dynamic system of the damped satellite with partially-filled liquid exhibits a rich variety of non-linear behaviours as certain parameters are varied. Due to the effect of non-linearity, regular or chaotic motions may occur. In this paper, both analytical and computational methods have been employed to study the dynamical behaviors of the non-linear system.

The stability conditions for the system have been found by using the Lyapunov direct method and a codimension one bifurcation analysis for the autonomous system is studied by using center manifold theory.

The periodic, and chaotic motion of the nonautonomous system are obtained by the numerical methods such as power spectrum, the Poincaré map and Lyapunov exponents. All these phenomena have been displayed in bifurcation diagrams. More information of the behaviors of the periodic and the chaotic motion can be found in parametric diagrams. The changes of parameter play a mojor role for the nonlinear system. Chaotic motion is the motion which has a sensitive dependence on initial condition in deterministic physical systems. The chaotic motion has been detected by using Lyapunov exponents and Lyapunov

dimensions. Besides, a global analysis of the non-linear system have been obtained by using modified interpolated cell mapping (MICM).

The presence of chaotic behavior is generic for suitable non-linearities, ranges of parameters and external force, where one wishes to avoid or control so as to improve the performance of a dynamical system. Several methods are used to control chaos effectively.

By using a number of analytical or computational methods, the non-linear behaviors of the satellite like the different types of periodic solutions, the effects on the solutions caused by different parameters and initial conditions, and the stability analysis of solutions have been studied here. In spite of the difference between these methods, the results obtained agree well. The conclusion is that there exist complicated phenomena in the dynamics of the non-linear system.

ACKNOWLEDGMENT

This research was supported by the National Science Council, Republic of China, under Grant Number NSC 85-2212-E-009-014.

REFERENCES

1. F. C. Moon 1992 *Chaotic and Fractal Dynamics*. New York: Wiley.
2. H. K. Khalil 1996 *Nonlinear Systems*. Englewood Cliffs, NJ: Prentice-Hall.
3. Z.-L. Wang 1992 *Stability of Motion and its Application*. Mainland: Publishing house of high education (Chinese).
4. I. G. Malkin 1952 *Theory of Stability of Motion*. Moscow—Leningrad: Translated from a publication of the state publishing house of Technical-Theoretical Literature.
5. J. Guckenheimer and P. J. Holmes 1983 *Nonlinear Oscillations of Dynamical Systems and Bifurcations of Vector Fields*. New York: Springer.
6. B. D. Hassard, N. D. Kazarinoff and Y.-H. Wan 1981 *Theory and Applications of Hopf Bifurcation*. Cambridge: Cambridge University Press.
7. J. Carr 1981 *Applications of Center Manifold Theory*. New York: Springer.
8. H. Poincaré 1892 *Les Méthodes Nouvelles de la Mécanique Céleste*. Paris: Gauthier–Villars.
9. S. Wiggins 1990 *Introduction to Applied Nonlinear Dynamical Systems and Chaos*. New York: Springer.
10. A. Wolf, J. B. Swift, H. L. Swinney and J. A. Vastano 1985 *Physica* **16D**, 285–317. Determining Lyapunov exponents from a time series.
11. J. Wright 1984 *Physical Review A* **29**, 2924–2927. Method for calculating a Lyapunov exponent.
12. P. Frederickson, J. L. Kaplan, E. D. Yorke and J. A. Yorke 1983 *Journal of Differential Equations* **49**, 185–207. The Lyapunov dimension of strange attractors.
13. Z. M. Ge and S. C. Lee 1997 *Journal of Sound of Vibration* **199**, 189–206. A modified interpolated cell mapping.
14. S. Sinha, R. Ramaswamy and J. S. Rao 1991 *Physica D* **43**, 118–128. Adaptive control in nonlinear dynamics.
15. Y. Braiman and I. Goldhirsh 1991 *Phys. Rev. Lett* **66**, 2545–2548. Taming chaotic dynamics with weak periodic perturbations.
16. E. Ott, C. Grebogi and J. A. Yorke 1990 *Phys. Rev. Lett* **64**, 1196–1199. Controlling chaos.
17. B. A. Huberman and E. Lumer 1990 *IEEE Transaction on Circuits and Systems* **37**, 547–550. Dynamics of adaptive system.